Sensitivity of planktonic foraminifera to Pleistocene climate change in the SE Atlantic

Ufkes, E.

2010

document version
Publisher's PDF, also known as Version of record

Chapter 7

Concluding remarks: Southern hemisphere paleoceanography in a global climate change context during the Mid-Pleistocene Transition

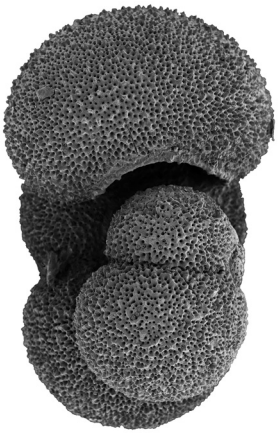

E. Ufkes and D. Kroon

Abstract

In this chapter, the foraminiferal faunal patterns of Core T89-40 are placed in a global palaeoceanographic context. The surface waters of the core location are influenced by the extent of the subtropical gyre versus the Benguela Upwelling System, in turn driven by a complex interaction between atmospheric circulation patterns. The planktonic foraminiferal record of Core T89-40 shows that maximum extent of the subtropical gyre at the expense of the Benguela upwelling system occurred during maximum boreal insolation, whilst planktonic foraminiferal records from South of Africa, Southern Ocean and the deuterium record of Dome C Antarctica show increased warming of the southern hemisphere at the same time. We attribute these periods of general warming in the southern hemisphere to increased poleward heat transport in response to intense Hadley cell circulation driven by orbital Milankovitch cycles. Tilt cycles (41 ky) are important throughout the planktonic foraminiferal record of Core T89-40, whilst the eccentricity cycle, 100 ky, became dominant during about the last 650 ky. This shift towards a dominant 100 ky cycle in surface water changes in the S-Atlantic is congruent with ice volume changes during the Mid-Pleistocene Transition.

Introduction

In chapters 5 and 6, I presented the planktonic foraminiferal abundance patterns of Core T89-40, SE Atlantic over the past 1.1 million years. These planktonic foraminiferal abundance patterns show the SE Atlantic water mass movements for the last 1.1 million years. Most of the variation in the abundance patterns as expressed in PC 1 (Figure 7.1) can be explained by the cyclical presence of oligotrophic, warm gyre waters versus eutrophic, cold upwelling waters through time.

The cyclical nature of the abundance patterns suggests that water mass movements were driven by processes influenced by orbital insolation cycles.. Statistical analysis showed that most variability in this subtropical SE Atlantic record is congruent with the northern hemisphere insolation record (Table 7.1). This suggests that the main SE Atlantic oceanic surface water mass lateral movements in the southern hemisphere were controlled by northern hemisphere climate processes, but how? In this chapter, I make an attempt to place the Core T89-40 results in an Atlantic – global climate context and make an attempt to understand which northern hemisphere processes, driven by insolation, are key to the understanding of southern hemisphere paleoceanographic changes.

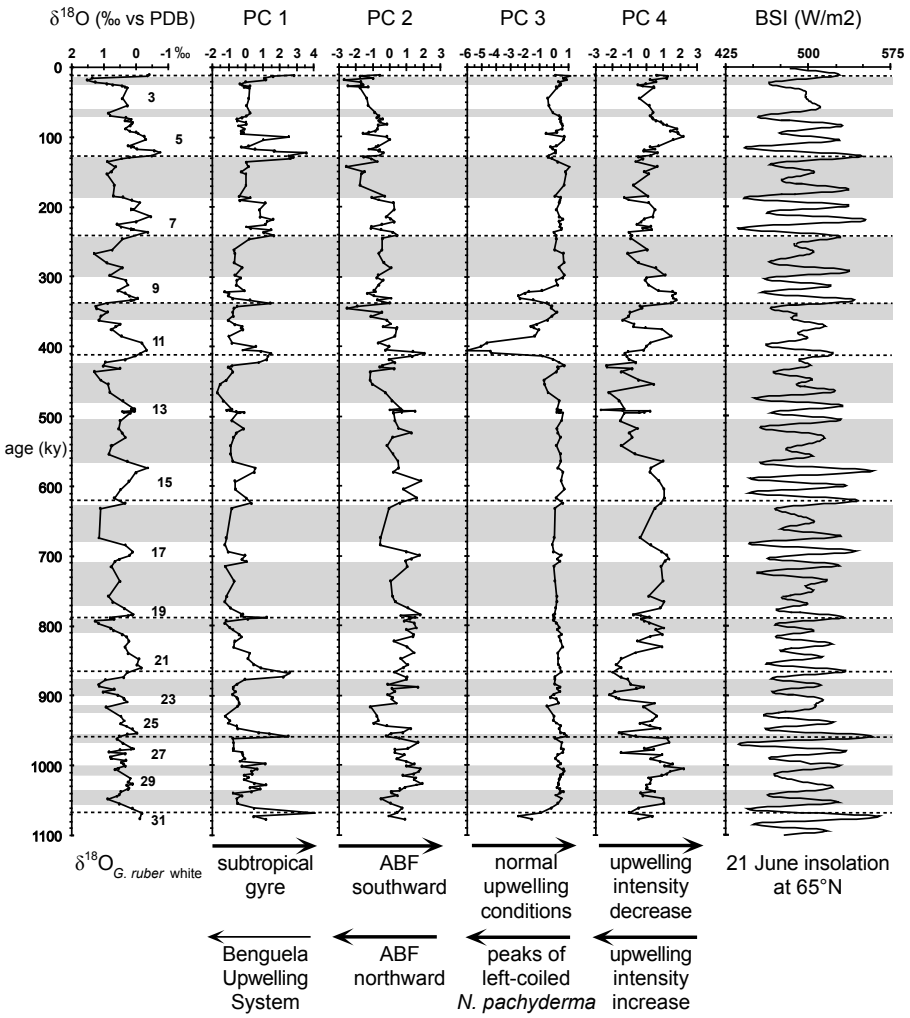

Figure 7.1
The downcore distribution of the oxygen isotope stratigraphy and the 4 principal components; the maximum daily insolation at 65°N at June 21st (BSI) using the Berger 1978 solution (Analyseries; Berger, 1978; Paillard et al., 1996). Glacial periods are shaded grey. Numbers refer to marine isotopic stages. PC 1 depicts subtropical gyre waters versus upwelling filaments from the Benguela Upwelling System. PC 2 reflects the change in position of the Angola-Benguela Front (ABF): positive values represent southward shifts of the Angola-Benguela Front. Strong negative values of PC 3 reflect extreme upwelling events indicated by peaks of left-coiled *N. pachyderma*, whereas positive values of PC 3 point to more normal upwelling conditions. PC 4 points to the upwelling intensity. A decrease in upwelling intensity, positive values, are also affected by a southward shift of the Angola-Benguela Front. The line thickness of the arrows corresponds to the main loading of the principal components. The dashed lines denote peaks in PC 1 during MIS 1, 5, 21, 25 and 31, which match the maxima in insolation.

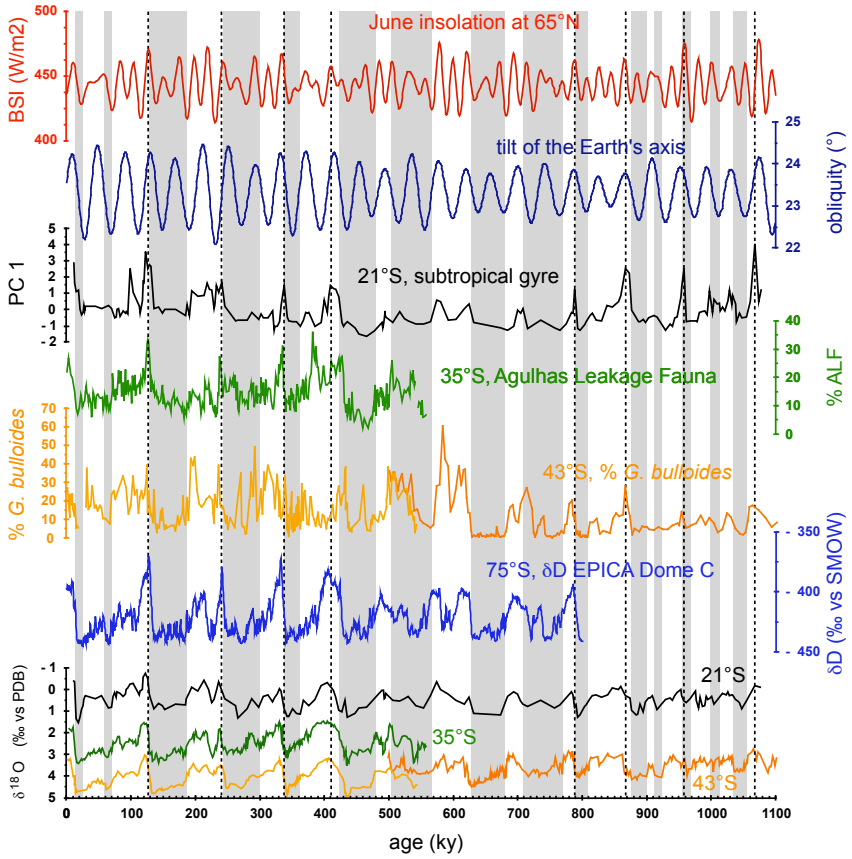

Figure 7.2
Long-term changes in insolation, obliquity, temperature sensitive foraminiferal parameters, and oxygen isotope records:
- 21 June insolation at 65°N (Berger, 1978); - Variation in obliquity or tilt of the Earth's axis (Berger, 1978); - Scores of the subtropical gyre principal component (PC 1) at Core T89-40 (21°36'S, 6°47'E); - Relative abundances of the warm Agulhas Leakage Fauna in the Cape Basin record which is a composite of GeoB 3603-2 and MD-96-2081 (35˚08'S, 17˚33'E; 35˚21'S, 17˚25'E) (Peeters et al., 2004); - Relative abundances of *Globigerina bulloides* at PS2489-2 and ODP Site 1090 (42°52'S, 08°58'E; 42°55'S, 8°54'E) revealing 'warm' periods (Becquey and Gersonde, 2002); - Deuterium isotopes at EPICA Dome C Ice Core (75º06'S, 123º21'E) (Jouzel et al., 2007); - Oxygen isotope records of *Globigerinoides ruber* white in Core T89-40 and of *Cibicidoides wuellerstorfi* in the Cape Basin composite core and ODP Site 1090 (Peeters et al., 2004; Becquey and Gersonde, 2002; this thesis). Glacial periods are shaded in grey. Age models as published have been used.

Correlation variability in time

	time slice (ky)	PC 1	PC 2	PC 4	trunc-r	trunc-l	$\delta^{18}O$	BSI	pb	FI
PC 1	11-400		0.23	0.007	0.265	**-0.466**	**-0.457**	**0.387**	0.215	-0.286
	200-600		0.29	0.104	**0.412**	-0.157	**-0.421**	**0.272**	**0.45**	**-0.563**
	400-800		**0.286**	-0.099	0.107	0.015	**-0.428**	**0.25**	**0.391**	**-0.441**
	600-1000		0.159	**-0.372**	0.033	-0.063	**-0.331**	**0.268**	**0.466**	**-0.5**
	800-1078		0.158	**-0.275**	-0.15	0.068	**-0.431**	0.172	**0.315**	**-0.342**
	961-1078		0.144	-0.281	-0.127	-0.003	**-0.57**	0.007	0.231	**-0.558**
PC 2	11-400	0.23		0.111	0.031	0.13	**-0.512**	**0.305**	-0.016	0.152
	200-600	0.29		-0.148	0.074	-0.063	**-0.475**	0.23	0.173	-0.018
	400-800	**0.286**		**0.333**	0.132	0.106	**-0.3**	0.135	**0.237**	**-0.267**
	600-1000	0.159		**0.283**	0.162	0.149	-0.142	-0.121	0.22	**-0.319**
	800-1078	0.158		**0.315**	-0.003	**0.374**	-0.21	**-0.274**	0.001	-0.108
	961-1078	0.144		0.331	-0.061	**0.403**	-0.31	-0.217	-0.06	-0.077
PC 4	11-400	0.007	0.111		**0.594**	-0.129	**-0.275**	0.064	0.193	0.112
	200-600	0.104	-0.148		**0.258**	-0.027	**-0.251**	-0.153	**0.322**	**-0.376**
	400-800	-0.099	**0.333**		0.101	-0.001	0.021	-0.042	-0.047	0.118
	600-1000	**-0.372**	**0.283**		0.132	0.222	0.103	-0.055	**-0.336**	**0.428**
	800-1078	**-0.275**	**0.315**		-0.047	**0.337**	0.097	-0.006	**-0.502**	**0.638**
	961-1078	-0.281	0.331		-0.196	-0.139	0.197	0.061	**-0.382**	0.348

Table 7.1
Pearson correlation variability in time; 400-ky time windows in steps of 200 ky as well as the period prior to the Mid-Pleistocene Transition (> 961 ky): principal components PC 1, PC 2 and PC 4, percentages of *G. truncatulinoides* right-coiled (trunc-r), *G. truncatulinoides* left-coiled (trunc-l), oxygen isotopes of *G. ruber* white ($\delta^{18}O_{rw}$), 21 June insolation at 65°N (BSI), plankton-benthos ratio (PB = p/(p+b)) and fragmentation index (FI) in steps of 400 ky. Bold numbers represent correlation coefficients significantly different from zero using a 95 % confidence level.

The cyclical nature of the abundance patterns suggests also that ice volume changes may have played a role in southern hemisphere paleoceanographic changes. The orbital cycles triggered ice volume changes which were dominant in Pleistocene climate change (e.g. Hays et al., 1976). Glacial-interglacial climate variability, ice volume changes, have been attributed to changes in boreal summer insolation. The dominant frequency of ice volume changes, however, showed an important change in rhythm around 960 ky during the Mid-Pleistocene Transition (MPT). The dominance of the 41-ky cycle diminished whilst the 100-ky cycle became very prominent in the late Pleistocene. This can be clearly seen in the stable isotope records of Core T89-40 based on planktonic foraminiferal shells (Figures 5.2 and 7.2). These ice volume changes in the northern hemisphere may have left their imprint on the southern hemisphere paleoceanography through atmospheric or oceanographic connections. But which connections were important, and were these connections similar in origin for insolation and ice volume changes?

In Figure 7.2 I have plotted the main Core T89-40 subtropical planktonic foraminiferal abundance changes (as shown in PC 1 scores), other 'warm' planktonic foraminiferal abundance records and deuterium isotopes from

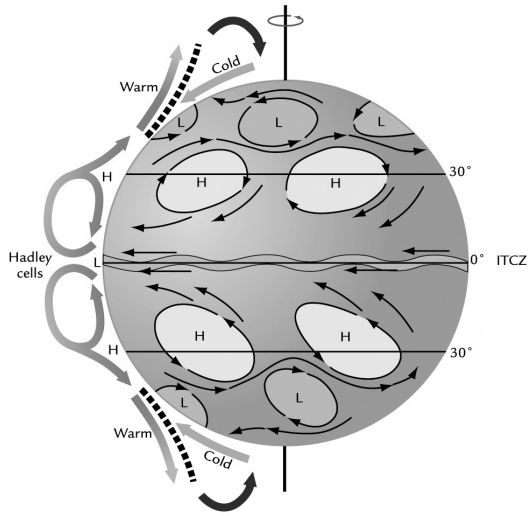

Figure 7.3
Schematic representation of the general circulation of the atmosphere. Heated air rises in the tropics at the ITCZ and descends in the subtropics as part of the Hadley cell circulation which transports heat away from the equator (after Ruddiman, 2001).

southern latitudes (e.g. those from cores at 35°S, 43°S and 75°S, composite cores GeoB 3608-2/MD96-2081, PS2489-2/ODP Site 1090 and EPICA Dome C), to present an overview of SE Atlantic paleoceanographic changes. The foraminiferal changes in Core T89-40 vary in phase with the changes in the records of the more southern located sites at the orbital time-scale. The fauna of the subtropical gyre positively varies with maximum peaks of (sub)tropical fauna south of Africa (the so-called Agulhas Leakage Fauna; Peeters et al., 2004) and with maximum peaks of the *Globigerina bulloides* record further south (these peaks record also relatively warm water in the Southern Ocean at ODP Site 1090; Becquey and Gersonde, 2002). These combined records show that the various southern hemisphere oceanic realms, which are connected by coupled main fronts and wind systems, responded similarly or were systematically linked to climate change through time. During reduced upwelling and increased influence of subtropical gyre waters in the SE Atlantic the Subtropical Convergence (STC) front shifted significantly southwards, resulting in warming in the southern hemisphere. The poleward extent of these shifts of warm waters concurred with maxima in boreal summer insolation at 65°N (BSI); the maximum daily insolation at June 21st at 65°N.

How to explain the simultaneous response of southern hemisphere oceanic changes driven by northern hemisphere insolation changes? Perhaps insolation variability may have directly influenced atmospheric circulation patterns which drive ocean currents, or insolation variability may have forced other components in the climate system such as ice volume and greenhouse gases, which in turn may have driven southern hemisphere oceanic changes?

Atmospheric circulation

One of the important phenomena in low latitude climate, and directly sensitive to insolation changes, is the Intertropical Convergence Zone (ITCZ) (Chiang, 2005). The ITCZ is a circum-global atmospheric belt of low atmospheric pressure, with intense, moist convection and rainfall, marking the convergence of northern and southern trade winds. The ITCZ comprises the rising branch of the Hadley cells (Figure 7.3) (Koutavas and Lynch-Stieglitz, 2005). The position of the ITCZ is distorted due to differential heating and cooling of land masses and oceans, whereas its interhemispheric mean position varies seasonally.

The subsiding branches of the Hadley cells, which occur in the subtropics at about 30°N and 30°S, form high-pressure zones (Figure 7.3). The subsiding branches are important, however, for bringing tropical heat to higher latitudes. In general, the Hadley cell circulation represents large scale atmospheric overturning driven by insolation and latitudinal temperature gradients (Lindzen and Hou, 1988; Rind and Perlwitz, 2005; Webster, 2005; Broccoli et al., 2006).

The Hadley cell circulation is sensitive to insolation patterns throughout the year, particularly seasonal effects are manifested in the position of the ITCZ and intensity of the atmospheric overturning, all directly important for the heat distribution on Earth. The ITCZ follows insolation maxima and migrates from the southern tropics in austral summer to the northern tropics in boreal summer. An associated strong Hadley cell circulation develops in the opposing cool, winter hemisphere (Lindzen and Hou, 1988; Broccoli et al., 2006). This is schematically represented in figures 7.4 and 7.5.

Various studies suggest that variations in equatorial insolation could induce anomalous tropical sea surface temperatures which determine the strength of the Hadley circulation (Ashkenazy and Gildor, 2008) and position of the Subtropical Convergence (Bard and Rickaby, 2009). During glacial periods Chylek and others (2001) hypothesize that the Hadley cell is contracted and confined closer to the equator due to lower tropical sea surface temperatures. However, modeling studies by Rind and Perlwitz (2005) suggest that the poleward extent of the Hadley cell is not strongly related to equator-to-pole temperature gradient. The meridional temperature gradients through time may vary due to global climate processes, e.g. ice volume, which in turn may be dependent on insolation variation.

The seasonal effects on the meridional position of the Hadley cell and intensity as a function of rotation of the Earth around the sun can be summarised as follows. During the equinoxes (March, September) the Hadley circulation is marked by two relatively weak symmetric cells with the ITCZ near the equator (Figure 7.5a). During the solstitial seasons (marked by maximum seasonal

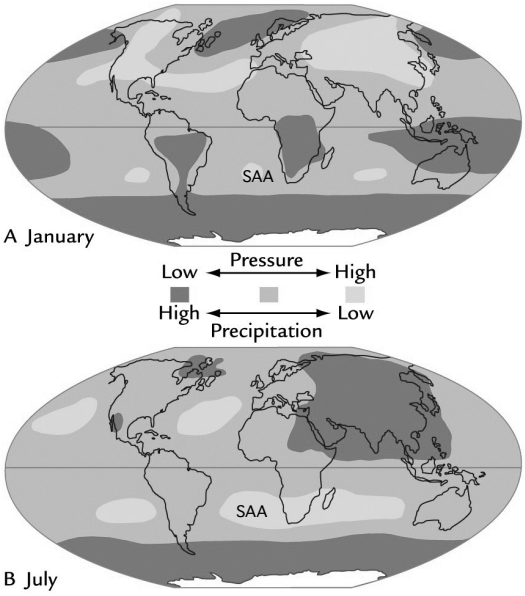

Figure 7.4
Schematic representation of the seasonal pressure patterns (after Ruddiman, 2001). In austral winter, the SH is marked by a zone of high surface pressures in the subtropics connecting the S. Atlantic and Indian Ocean high-pressure systems. During austral summer, this band is interrupted by an area of low pressure on the African continent. Differential heating of land masses and oceans results in seasonal transfer of heat between tropical land and ocean, the monsoonal circulation. The areas of maximum high-pressure are indicated by "SAA"; during austral summer the SAA is located at 32°S 5°W, during austral winter at 27°S 10°W (Peterson and Stramma, 1991).

differences between northern and southern hemisphere; June, December) a much stronger cross-equatorial cell develops in the coldest, the winter hemisphere with rising motion in the tropics and widespread descending air in the winter hemisphere redistributing heat from the tropics to the poles (Figures 4b and 4c) (Lindzen and Hou, 1988; Webster, 2005). Thus during a northern hemisphere summer, a strong Hadley cell accompanied by a strong high-pressure zone will develop in the opposing southern hemisphere (Figure 7.5c).

Seasonal extremes are perhaps key to the redistribution of heat in either hemisphere. During a solstice the tilt of the Earth's axis, or obliquity, is most inclined toward the sun. Theoretically periods with maximum tilt of the Earth's axis should lead to seasonal extremes in both hemispheres, which renders the orbital tilt cycle (about 41 ky) important, because it changes the angle of tilt through time. The other orbital cycle of precession (about 21 ky), further

modulates seasonality, particularly the timing of the seasonal extremes. This is reflected by the 21-ky cyclicity in the BSI.

Subtropical gyre

Intensified southern hemispheric Hadley circulation may affect the poleward extent of the subtropical gyre. The currents driving the subtropical gyre are affected by the trade winds and westerlies. The trade winds result from the atmospheric circulation related to the South Atlantic Anticyclone high pressure system (SAA) and the equatorial low pressure area (Figure 7.4) (Wefer et al., 1996). In the S. Atlantic the SAA is connected to the southern edge of the Hadley cell.

During the austral winter, the SAA is more strongly developed and situated to the northwest (27°S 10°W). This results in intensification of SE trade winds. During austral summer the SAA is located more to the southeast (32°S 5°W; Peterson and Stramma, 1991). However, the development of SE trade winds is also affected by the development of thermal lows over the South American and South African continents due to differential heating of land and sea. During austral summer pressure differences between land and sea are larger isolating the SAA and reducing seasonal upwelling in the northern Benguela Upwelling System (BUS). In the northern BUS maximum upwelling intensity, which affects the hydrography at the core location, occurs during late winter and spring (Dingle and Nelson, 1993). In the southern BUS stronger trade winds result in a strengthening of the perennial upwelling (Peterson and Stramma, 1991). Figure 7.4 shows that although the SAA is located further south during the austral summer, the region of high-pressures is wider during austral winter (Figure 7.4). Therefore, during austral winter (boreal summer) the subtropical gyre has its largest extent.

Intensified southern hemisphere Hadley circulation may have affected the poleward extent of the subtropical gyre. Subsequent increased poleward heat transfer may have attributed to the warming of the SE Atlantic, the Southern Ocean and eventually the Antarctic region (Figure 7.2). The heat transport may have occurred during Pleistocene climate extremes driven by maxima in BSI and/or maxima in obliquity. Peak abundances of the subtropical gyre assemblage especially occur when maxima in boreal insolation and tilt coincide.

Impact of orbital forcing

The orbital cycles of tilt and precession determine the timing of extreme warm boreal summers during which more heat may have been transported to the south. Periods of increased warm boreal summers as indicated by peak

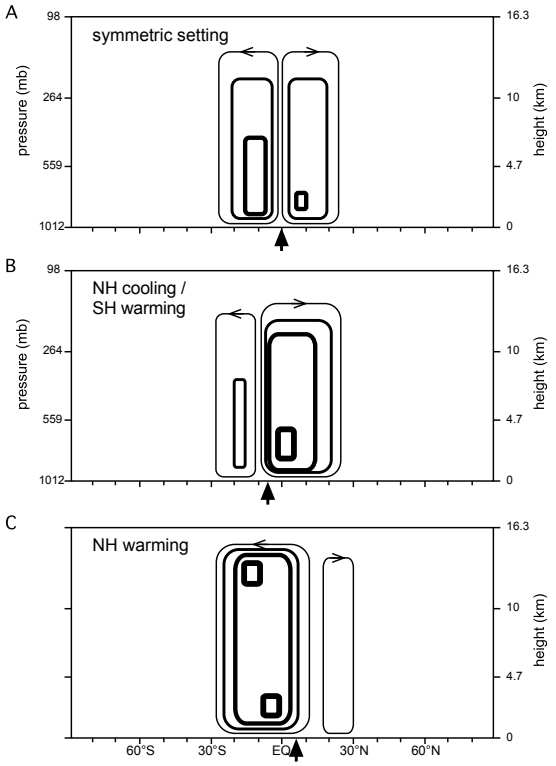

Figure 7.5
A schematic latitude-height cross section of annually averaged meridionally stream function of the Hadley cell circulation after model results of various temperature patterns (Lindzen and Hou, 1988; Broccoli et al., 2006).
A - a symmetrical temperature pattern, e.g. during equinoxes (after Broccoli et al., 2006).
B – an asymmetric temperature pattern due to northern hemisphere (NH) cooling and southern hemisphere (SH) warming. A reduced heat flux of 10 W/m^2 north of 40°N concurrent with an enlarged heat flux of 10 W/m^2 south of 40°S results in a 6° southward shift of the ITCZ and an intensification of the NH winter cell (after Broccoli et al., 2006).
C – an asymmetric temperature pattern due to SH cooling. An ITCZ shift of 6° northwards results in an intensification of the SH winter cell (after Lindzen and Hou, 1988).
Lines broaden with increasing stream function.

abundances of the subtropical gyre assemblage (expansion of the gyre at the expense of northern BUS upwelling waters) generally concur with phases of maximum tilt of the Earth's axis (Figure 7.2). Extension of the gyre and the southward shifts of the main fronts occurred at the same time, synchronous with the periods of maximum tilt, implying maximum seasonality may have been an important factor in driving heat southwards through an intense southern hemisphere Hadley cell.

Another interesting correlation can be made between periods of maxima in the warm water signals in the southern hemisphere and insolation. In Figure 7.2, the timing of maxima in warm water signals in the southern hemisphere correlates well with maximum northern summer insolation, particularly the most outstanding peaks. This correlation strongly hints that tilt and precession played an important role, but the fact that northern hemisphere insolation played a role in such scenario rather than southern hemisphere insolation is curious. During maximum tilt both the Northern and the southern hemisphere are affected and may show a concurrent increase in "warm" southern hemisphere parameter and northern hemisphere insolation on an annual basis. Precession will result in an opposing seasonal insolation trends in both hemispheres. Boreal summer insolation increases when the northern hemisphere June solstice occurs when the Earth is closest to the sun (perihelion).

Ice volume changes: Interglacial and glacial settings

Insolation may also have driven other processes in the S. Atlantic that were important in SH heat distribution variability. Maximum interglacial conditions marked by higher Boreal Summer Insolation (BSI) correlate also with reduced ice volume in the world. Glacial-interglacial climate variability, ice volume changes, have been attributed to changes in BSI. The various warm peaks precede minima in $\delta^{18}O$, a ice-volume proxy, but they are in phase with obliquity. Fluctuations in Antarctic ice volumes show a strong pacing by obliquity; minima in obliquity resulted e.g. in maximum extent of the Antarctic ice sheets (Naish et al., 2009). A subsequent equatorial shift of the polar front system will directly affect the various warm water peaks in the S. Atlantic. Insolation appears to have a more direct response in the S. Atlantic warm water signals than the assumed time lag of about 3.6 ky in a 100-ky forcing between insolation and ice volume (Imbrie et al., 1993). Studies by Naish and others (2009), however, do not show a clear time lag between obliquity, insolation and ice volume.

Interglacial setting

Previous interglacial periods are best compared with the modern atmospheric circulation with minimum ice-sheet extent. Maximum interglacials conditions marked by a high BSI and light $\delta^{18}O$ concur with minimum precession (maximum boreal insolation) although today the Northern Hemisphere June solstice is close to the aphelion position, maximum tilt (amplifying seasonal differences) and minimum eccentricity. During insolation maxima at 65°N also (Antarctic) sea-ice retreated resulting in a more poleward position of the polar

frontal system including the STC, generating enhanced Agulhas leakage as well as higher sea surface temperatures at 43°S and higher temperatures in Antarctica (Figure 7.2). Prior to 900 ky the maximum extent of the subtropical gyre (high scores of PC 1) shows a clear 41-ky cyclicity (Figures 5.5 and 7.2). Obliquity had an apparent stronger impact on the seasonal insolation than the 100-ky cyclicity prior to 900 kyr.

Glacial setting

During glacial periods with increased sea-ice extent thermal gradients have steepened and intensified the trade winds and hence gyre circulation. Further, the southern polar fronts and subtropical convergence (STC) will shift equatorwards. Giraudeau and others (2002) also suggested an accompanying equatorward shift of the atmospheric high pressure cell (SAA) and main center of upwelling in the Benguela Upwelling System (BUS). This outcome would fit the results and hypotheses by Chylek and others (2001) and Bard and Rickaby (2009). However, models by Rind and Perlwitz (2005) showed no clear relation of the poleward extent of Hadley cells to mean temperature or equator-to-pole temperature gradient. Since about 900 ky, not every peak in BSI is reflected in the SE Atlantic warm water faunas. Extensive ice sheets may have dampened the temperature effect of maximum insolation at 65°N resulting in less intense southern hemisphere high pressure zone and increased upwelling and subsequent a less eastward extent of the subtropical gyre with respect to the core location. Reduced glacial heating of the continent will also weaken the land-sea pressure gradient increasing trade winds and subsequent upwelling in the northern BUS.

Paleoceanographic changes during the MPT

The temporal matching of the peaks of maximum heat in the southern hemisphere with peaks in maximum BSI is visible throughout the entire record, whereas matching with maxima in obliquity is best during early and middle Pleistocene (Figure 7.2). The stable isotope records indicate the glacial-interglacial cycles throughout the record with a clear change in dominance of the 41-ky cycle to the 100-ky cycles during the Mid-Pleistocene Transition (MPT) (Figure 5.5). The 100-ky cyclicity, that was initiated at about 900 ky ago by a pulse in ice-sheet extent, became dominant after about 650 ky, at the end of the MPT.

It is interesting to note that during the MPT various changes in low-latitudinal atmospheric and oceanic circulation occurred as evidenced in other records: 1) a change in the origin of marine productivity (Schefuß et al., 2005); 2) a

change in the precipitation pattern in time (Dupont et al., 2001); 3) a "reversed" behaviour of the thermocline in the western equatorial Atlantic (Cullen and Curry, 1997); 4) "trapped" heat (increased glacial Sea Surface Temperatures) in the Angola Basin (Schefuß et al., 2003; Schefuß et al., 2004). All of the above mentioned studies point to a southern hemisphere climate response near the MPT triggered by ice volume changes.

At Walvis Ridge in the SE Atlantic, these low-latitudinal atmospheric and oceanic circulation changes also had an impact on the southward extent of Angolan waters (PC 2), the Benguela Upwelling System (BUS; PC 4) as well as evolutionary changes in *Globorotalia truncatulinoides* (see chapter 5). At Core T89-40, the presence of warm Angolan waters started to diminish in favour of the extent of the subtropical gyre (PC 1) around 400 ky. The re-entry of left-coiled *G. truncatulinoides* at 610 ky was followed by a cyclic alternation of left- and right-coiled *G. truncatulinoides* in line with glacial-interglacial cycles. All of these low latitudinal and Walvis Ridge events suggest not only change in the trade winds intensity, but also a change in African monsoonal circulation during the MPT.

A change in correlation between the extent of the subtropical gyre and BUS (Table 7.1) may result from a change in atmospheric circulation; an apparent concurrent maximum extent of both systems prior to 800 ky, whereas they alternate since 800 ky. The expansion of more dynamically responding North American ice sheets compared to the larger Eurasian ice sheets (Bintanja and van de Wal, 2008) will have had its impact on the differential heating of land and sea and therefore the North African monsoon. In the 100-ky world, the low-pressure area over (southern) Africa strongly affects the atmospheric circulation and resulting trade winds generated around an isolated SAA (Figure 7.4). The trade winds and subsequent upwelling were intensified during glacial periods related to an increase of the meridional pressure gradient (Little et al., 1997; Stuut et al., 2002b). Apparently prior to 800 ky these low pressure areas were less persistent generating smaller differences in seasonal pressure patterns. During this period increased trade winds were likely moreover linked to the season with the highest pressures, during boreal summer. Prior to 870 ky foraminifera derived summer sea surface temperatures of glacial and interglacial periods point to temperatures that characterize the present-day Polar Front Zone implying a northward shift of isotherms by about 7° of latitude (Becquey and Gersonde, 2002). Further, a more equatorward position of polar fronts compared to the modern setting will have strengthened thermal gradients and subsequent trade wind and upwelling intensity during early Pleistocene interglacials periods.

Glacial periods prior to 800 ky as recorded in the proxy records of Core T89-40, are marked by a reduced upwelling suggesting weakened meridional thermal gradients. At ODP Site 1090 glacial-interglacial variation in oxygen

isotopes of benthic foraminifera and foraminifera derived summer Sea Surface Temperatures remained limited prior to 650 ky and even more prior to 870 ky (Becquey and Gersonde, 2002), suggesting reduced variability in the position of polar fronts and STC. Even though only limited glacial cooling of tropical regions occurred (Schefuß et al., 2004), temperature variations in the subantarctics were even smaller. Prior to 870 ky, glacial-interglacial temperature variability was limited to about 2°C compared to 7°-11°C at ODP Site 1090 during the L. Pleistocene. In the tropics temperature variability was about 3° and 5°C respectively. This resulted in less intense subantarctic-tropical thermal gradients and subsequent northern BUS upwelling during these glacial periods. This apparent 'reversed' pattern in trade wind intensity may also have had its impact on the thermocline dynamics in the equatorial Atlantic.

Conclusions

(1) The SE Atlantic paleoceanography largely mirrors the well known global climatic cycles, including the switch from 41-ky to 100-ky cycles during the Mid-Pleistocene Transition (MPT), driven by the changes in low to high latitude heat gradients. Maximum boreal summer insolation at 65°N affects via the Hadley cell circulation the southern hemisphere warm water faunas during the past 1.1 million years. Obliquity largely modulates the seasonal insolation patterns as well as the ice-sheet extent in both hemispheres.

(2) In the S. Atlantic, the warm water signals are largely affected by the Hadley cell circulation driven by northern hemisphere summer insolation and are amplified by maxima in obliquity. Obliquity in turn also affects the Antarctic ice volume and subsequent the position of polar frontal systems. The resultant trade winds influence the Benguela upwelling intensity.

(3) The trade wind regime altered during the past 1.1 million years. At the end of the MPT, increased glacial-interglacial thermal variability in the subantarctic and the tropics strongly influenced thermal gradients and subsequent trade winds. Prior and during the MPT the trade winds and subsequent upwelling showed a "reversed" intensity pattern; increased trade winds during interglacial periods and reduced trade winds during glacial periods.

(4) Core T89-40 at crossroads of various distinct oceanographic realms provided a brief and simplified view of these processes. Future studies should include a more detailed and integrated approach on the impact of the low-latitudinal oceanographic and atmospheric circulation on the S. African, S. Atlantic and even Indian Ocean palaeo-oceanographic and palaeo-climatic records.